Pearling Instabilities of a Viscoelastic Thread

A. Deblais,[1] K. P. Velikov,[1,2] and D. Bonn[1]
[1]Van der Waals-Zeeman Institute, Institute of Physics, University of Amsterdam, 1098XH Amsterdam, Netherlands
[2]Unilever R&D Vlaardingen, Olivier van Noortlaan 120, 3133 AT Vlaardingen, Netherlands

(Received 15 November 2017; published 11 May 2018)

Pearling instabilities of slender viscoelastic threads have received much attention, but remain incompletely understood. We study the instabilities in polymer solutions subject to uniaxial elongational flow. Two distinctly different instabilites are observed: beads on a string and blistering. The beads-on-a-string structure arises from a capillary instability whereas the blistering instability has a different origin: it is due to a coupling between stress and polymer concentration. By varying the temperature to change the solution properties we elucidate the interplay between flow and phase separation.

DOI: 10.1103/PhysRevLett.120.194501

Pearling instabilites have been much studied; in the context of cell membranes they are associated with cell shape and cell division [1] and for artificial membranes, curvature-induced pearling instabilities have been associated with membrane heterogeneity and local phase separations [2]. Such pearling instabilities generally result from a complicated interplay between bulk and surface stresses, which are in some cases actively driven; therefore a complete understanding is still lacking. A much simpler model system that exhibits strikingly similar pearling instabilities is a polymer solution. Understanding and controlling the rheology of such solutions of especially high-molecular-weight polymers is crucial in numerous applications such as flow control in microdevices [3], fluidizing paint or concrete, and drop size control in pesticide spraying or ink jet printing [4–6]. These applications rely for a major part on the spectacular changes in extensional rheology that arise from the presence of small amounts of high-molecular-weight polymers. The generic way of investigating extensional viscosity is to look at the ensuing rupture of liquid columns [7–11]. Making a drop from an orifice leads to the formation of a slender cylindrical thread with an initially uniform thickness. In many cases the column destabilizes and its thickness becomes nonuniform; this is usually referred to as beads on a string (BOAS) [10,12–15], a droplike pattern created on a thin column of viscoelastic liquid. At the final stages of thinning, another pattern is sometimes observed [16–18] that is superficially similar, characterized by small droplets that form in between the initially formed beads on a string (blistering).

These thread instabilities received a lot of attention also because satellite beads are often undesired [8,12,16,19,20]. De Olivera and McKinley propose that a competition between elastic, capillary, and inertial forces leads to the formation of the beads-on-a-string structure, but that such a state is inherently unstable leading to successive instabilities in the necks connecting the beads and the ligaments [17]. The precise mechanism of both the primary and the secondary instability is however not understood. Clearly, the elastic forces generated by the stretching of the polymers impede the finite-time singularity that is present for Newtonian liquids [21]; however also for Newtonian fluids satellite drops are observed, so that the instability mechanism may be independent from the elastic forces [22,23]. The BOAS pattern is clearly not a simple Rayleigh-Plateau-like instability since the beads are very far apart [12]. The blistering instability could be a secondary instability leading to smaller beads on a thinner string; in this case, the mechanism should be similar to that of BOAS instability. However, recent theory [20] suggests a completely different mechanism based on a dynamical phase separation due to the coupling between local stress and local concentration in the liquid thread that remains to be tested experimentally.

Here we show that indeed the origin of the two instabilities is very different: the BOAS structure is controlled by an interplay between capillary and elastic forces, and induced by local symmetry breaking in the fluid neck. On the other hand, the blistering instability is due to a dynamical phase separation that takes place in the elongational flow. The latter is concluded from temperature-controlled experiments in which we compare two types of polymers in solution, one of which shows a phase separation at high temperatures [24,25]. Blistering is the dynamical precursor of the separation that takes place around the phase-separation temperature. The temperature of dynamical phase separation scales with the strain rate follows from a simple argument for the coupling of the flow with the phase separation. The control of temperature during drop formation consequently allows us to tune the different instabilities of a viscoelastic thread of polymer solution.

We study the extensional thinning and destabilization of filaments of long-chain polymer solutions in water at different concentrations. The experiments are performed with polyethylene oxide (PEO) of a molecular weight (M_w)

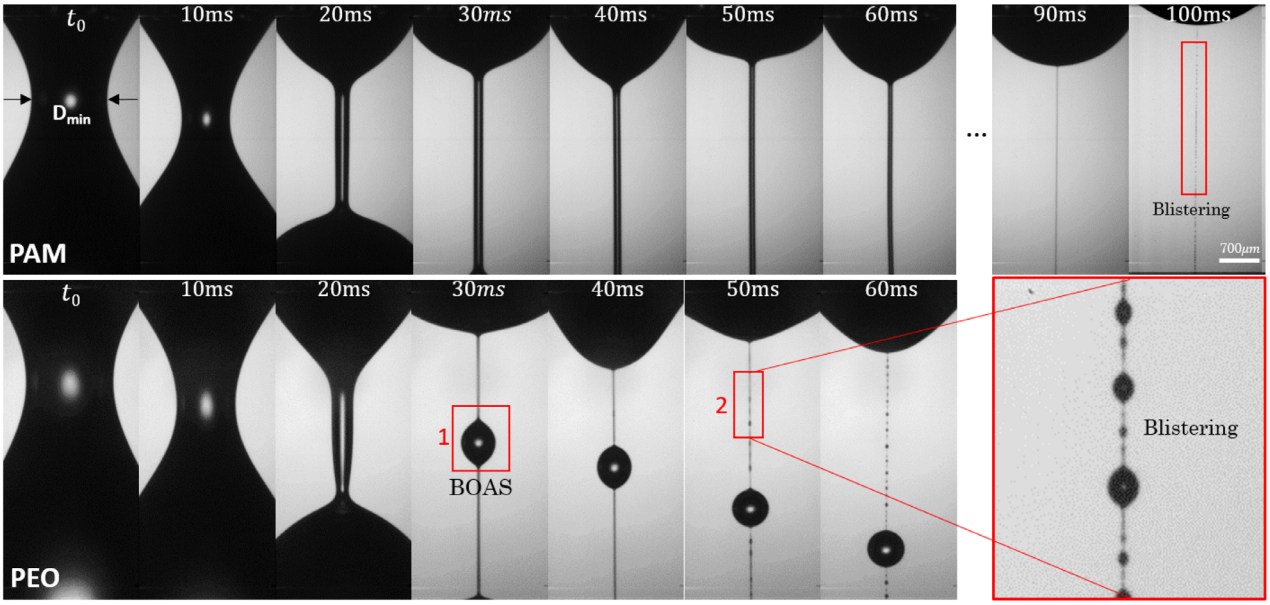

FIG. 1. Photographs of the breakup neck dynamics of PAM (upper panel) and PEO (lower panel) solutions at $T = 100\,°C$. At room temperature, both of these polymer solutions have a similar relaxation time λ_0. At higher temperatures, the breakup dynamics of PEO solution is modified due to phase separation. This leads to the formation of a satellite bead (1) at $t = 30$ms, followed by the formation of a nonuniform blistering pattern (2) at $t = 50$ms that appears sooner (or, e.g., at a larger neck diameter) than for the PAM solution. A closeup view of regime (2) is shown in the red frame.

of $4 \pm 2 \times 10^6$ g mol^{-1} [26] at concentrations $0.7 \leq c/c^* \leq 7$ and polyacrylamide (PAM) at $M_w = 15 \pm 6 \times 10^6$ g mol^{-1} [27] at concentrations $7 \leq c/c^* \leq 13$, both from Sigma-Aldrich (purity = 0.98). We use these because the ability to finely tune concentrations allows us to have comparable Zimm relaxation times λ_Z between the two polymers, and hence very similar flow properties. High molecular weight polymers invariably exhibit an important polydispersity, which may result in multiple time scales; however [12] showed that a single characteristic time is sufficient to describe the polymer flow dynamics. The Zimm time is calculated in the standard way: $\lambda_Z \cong [\{0.422[\eta]M_w\eta_s(T)\}/(N_a k_B T)]$ where $[\eta]$ is the intrinsic viscosity of the polymer solutions, N_A Avogadro's number, and k_B Boltzmann's constant. η_s is the viscosity of the solvent (with an exponential temperature dependence). A syringe pump supplies the polymer solutions to the needle tip (inner diameter $D_0 = 2$ mm); a high-speed camera with a microscope lens records the dynamics at 10,000 frames per second (see Supplemental Material Fig. 1, [28]). At room temperature, PEO and PAM show an initial thinning similar to that of a Newtonian fluid. Subsequently a very long and slender cylindrical filament is formed; in this elastocapillary thinning regime the dynamics slows down dramatically and follows $D_{\min} \propto e^{-t/3\lambda_0}$ with λ_0 being the longest relaxation time of the polymer solution [30]. At T = 20 °C, PEO and PAM exhibit similar thinning dynamics; the liquid columns are very stable and it is only at very late times that blistering appears (Supplemental Material Fig. 2). Quantitatively, the thinning rate and hence the elongational viscosity is the same: we find an almost identical relaxation time: $\lambda_{0,\mathrm{PEO}} = 3.1 \times 10^{-1}$ s and $\lambda_{0,\mathrm{PAM}} = 2.9 \times 10^{-2}$ s. However, at T = 100 °C (the solution does not boil because of boiling point elevation), PEO and PAM solutions show pronounced differences (Fig. 1): the latter shows dynamics similar to that at room temperature, with only a change due to the expected T dependence of the viscoelastic time scale. Only very close to filament breakup ($t = 100$ ms), formation of small blistering structures are observed. In contrast, PEO solutions are strongly affected by temperature and their dynamics changes qualitatively. There is almost immediate formation of a satellite bead [12–14] connected by two thin cylindrical threads: this is the BOAS structure (1). At later times, the filament rapidly becomes unstable ($t = 50$ ms) to form a strongly nonuniform blistering pattern (2) [16,17,20].

To gain insight into these surprising differences, Fig. 2 shows the T dependence of the relaxation times. For PAM this shows the predicted temperature dependence of the Zimm time: $\lambda_{0,\mathrm{PAM}} \sim \lambda_Z$ [see Fig. 2(c)]. For PEO, however, the relaxation time deviates strongly beyond T ~ 80 °C [Fig. 2(d)]: it becomes almost an order of magnitude smaller, and the deviation becomes more pronounced at high T; the strong T dependence is well described by $\lambda_{0,\mathrm{PEO}} \sim \lambda_p \propto e^{1/T}$ (Supplemental Material Fig. 4). Quantitative criteria for the formation of the satellite bead and the blistering structures are as follows. Reference [12] suggests that bead formation is due to a symmetry breaking in the filament: when necking occurs in the filament (usually close to the drop or the orifice),

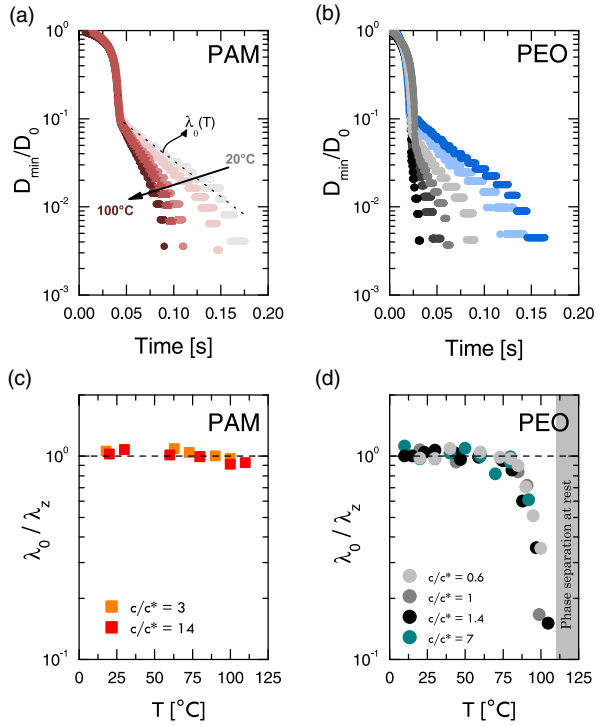

FIG. 2. Effect of temperature on the thinning dynamics. $D_{\min}/D_0$ is plotted as a function of time t for the case of (a) PAM and (b) PEO solutions. The relaxation times λ_0/λ_z of PAM (c) and PEO (d) of different concentrations $c/c*$ as a function of temperature T are deduced from the thinning curves. In the case of PEO solutions, the deviation becomes important for temperatures higher than 80 °C. The grey area shows the range of temperatures where the phase separation of PEO solution occurs at rest.

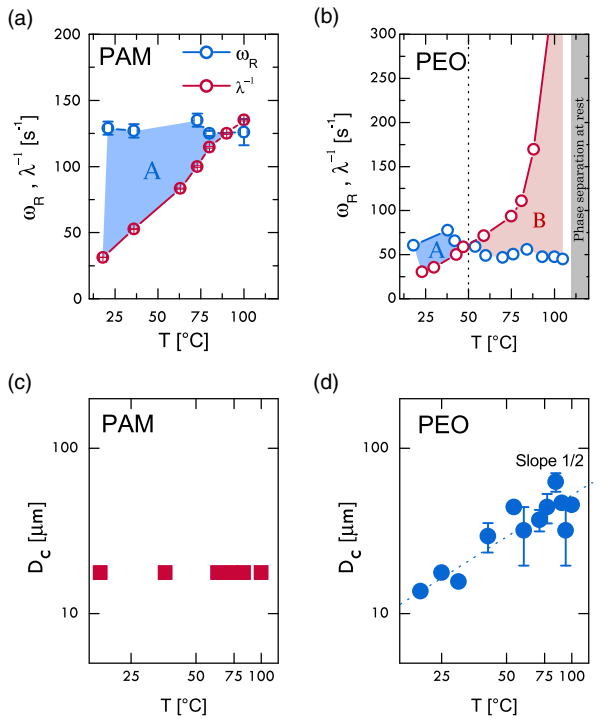

FIG. 3. BOAS is observed when the growth rate of the Rayleigh instability ω_R is smaller than the characteristic time of the polymer solution λ_0^{-1}. Domain A (blue) shows $\omega_R > \lambda_0^{-1}$ where no bead is observed. Domain B (red) is $\omega_R < \lambda_0^{-1}$, where a bead is formed on the filament. For PAM (a), no BOAS is observed for a wide range of temperatures, while PEO (b) shows a transition between domains $A \mapsto B$ at $T \sim 50\,°C$, giving rise to the formation of a bead (see Fig. 1, lower panel). Blistering appears for a critical neck diameter D_c. For PAM (c), the temperature does not affect the critical diameter, but for PEO (d), blistering is observed for a larger neck diameter when T increases.

the filament produces one or several beads. The symmetry breaking occurs for sufficiently strong deformations of the liquid filament. Comparing the experimental growth rate ω_R of the Rayleigh instability to λ_0, it follows that for PAM, the Rayleigh instability is simply not fast enough to produce a symmetry breaking and hence BOAS; Fig. 3(a) shows that $\omega_R > \lambda_0^{-1}$ for $T \leq 90\,°C$. For the last data point at the highest temperature we do not observe satellite beads and conclude that the two rates coincide to within the error. PEO shows satellite beads because the Rayleigh instability is fast enough, Fig. 3(b); this happens because of the strong temperature dependence of the relaxation time: around $T \sim 50\,°C$, $\omega_R < \lambda_0^{-1}$. This agrees quantitatively with the boundary between BOAS and no BOAS (Supplemental Material Fig. 5) and quantitatively accounts for the BOAS instability.

For the blistering, Figs. 3(c) and 3(d) show the critical diameter D_c at which the blistering appears. At room temperature, blistering starts for PEO at the same critical diameter as for PAM. However, as the temperature increases for PEO, blistering appears for increasingly larger values of D_c, which corresponds to a smaller capillary stress: the instability occurs much more readily. Quantitatively, Eggers [20] predicts that the coupling between polymer concentration and elastic stress sets this critical diameter, evaluated as $D_c = \sqrt{\Delta/\dot{\epsilon}} = \sqrt{3\Delta\lambda_0}$, with $\dot{\epsilon}$ being the stretching rate defined as $\dot{\epsilon} = 1/3\lambda_0$ (see Supplemental Material note 1 and Supplemental Material Fig. 3); $\Delta = k_B T/6\pi\eta_s(T)a$ is the diffusion coefficient with a being the polymer radius, with a temperature dependence that is the exact inverse of the Zimm equation. Taken together, this accounts for a temperature independent critical diameter $D_c = \sqrt{\Delta/\dot{\epsilon}}$. Hence, no temperature dependence is expected for D_c for PAM: the measured relaxation time has the same temperature dependence as Δ [Fig. 3(c)]. However for PEO solution the relaxation time strongly varies, and the temperature dependence is therefore expected to be $D_c \propto \sqrt{\Delta\lambda_p} \propto \sqrt{T}$. This agrees with the experimental data in Fig. 3(d): this quantitatively accounts for the blistering instability.

The main difference between PAM and PEO solutions is that the latter exhibit a macroscopic phase separation between a polymer-rich phase and a water-rich phase at

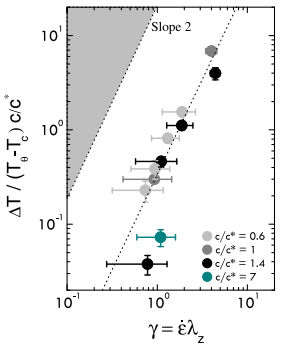

FIG. 4. The measured phase separation temperature shift ΔT as a function of the deformation $\gamma = \dot{\epsilon}\lambda_Z$ for PEO solutions of different concentrations c/c^*. The error bars represent the uncertainty on the measurements.

high T [31]. We determined the phase-separation temperatures visually by placing the solution in an oven and by slowly increasing the temperature (1 °C/day) until phase separation is observed (see Supplemental Material Fig. 6): $T_{sep} = 120\,°C$ for $0.6 \leq c/c^* \leq 1.4$ and $T_{sep} = 110\,°C$ for the higher concentration ($c/c^* = 7$), in agreement with [31]. The fact that important deviations in the thinning rate and instability formation are only observed close to the phase-separation temperature suggests that the coupling between the flow and the phase separation needs to be taken into account. There has been a massive amount of work on flow-induced phase separations in shear flow [32,33]; we borrow these arguments here and apply them to our elongational flow. Perhaps the simplest possible argument is that when polymer chains are deformed in flow, elastic energy is stored in those degrees of freedom, which increases the free energy of the homogeneous state. If there is no elastic energy stored in the phase-separated state, this naturally shifts the phase-separation temperature [34,35] by

$$|\Delta T| \sim (T_\theta - T_c)\frac{c}{c^*}\gamma^2,$$

where T_θ is the θ temperature [31], T_c the phase-separation temperature determined as mentioned above, c the polymer concentration, and c^* the overlap volume fraction. The deformation γ is the product of the deformation rate and the relaxation time of the polymer solution. The two lowest points seem to be slightly off the proposed scaling; perhaps this is due to them not yet being in the scaling regime. To compare with experiment, we quantify the difference in experimental relaxation time compared to the relaxation time predicted by Zimm (λ_Z). This difference can be translated into a shift in phase-separation temperature by simply assuming that the measured relaxation time in the flow corresponds to the Zimm relaxation time of the quiescent solution at a different temperature. The resulting temperature shift $\Delta T/(T_\theta - T_c)(c/c^*)$ is plotted in Fig. 4 as a function of the deformation $\gamma = \dot{\epsilon}\lambda_Z$, and exhibits the proposed scaling.

This then explains the much earlier formation of the blistering instability for PEO compared to PAM: the phase separation induced by the joint effects of temperature and extensional flow introduces inhomogeneities of polymer concentration in the polymer thread, thus giving rise to the formation of multiple beads on the polymer thread. The time scale of the instability was reported in [16]; the authors reported an inverse time scale $\omega^{-1} \approx 10$ ms. Eggers' theory [20] that we use predicts a time scale for the phase separation $\omega^{-1} \approx D_c^2/\Delta$; putting in values we also find $\approx$10 ms, so the two estimates agree. Our results also provide an explanation of earlier experiments [16,18] that showed that the thread rapidly becomes solid, implying that it is rich in polymer, whereas the blisters remain liquid and therefore are poor in polymer.

Because the temperature strongly affects the relaxation time of the PEO solution, it affects the BOAS instability also. Thus, BOAS always happens if the inverse of the relaxation time is large enough; this can also be achieved, e.g., by decreasing the polymer molecular weight or the concentration and is independent of any phase separation.

In conclusion, we studied the pearling instabilities of polymer threads for different polymers as a function of temperature. This control parameter allows us to elucidate the interplay between flow and phase separation. We show how the modified relaxation time of the polymer solution close to phase separation affects the instabilities. This is the bulk counterpart of the surface curvature induced instabilities in (artificial) membranes. For the polymer threads, our quantitative findings agree with the idea that BOAS and blistering instabilities have a very different physical origin, in spite of the fact that their manifestation—small drops on a thin filament—appears similar. Temperature is therefore an interesting parameter to control the appearance of different instabilities by controlling the interplay between the hydrodynamic, capillary, and elastic forces on the one hand, and phase separation on the other hand. These findings are potentially applicable to numerous industrial applications involving polymer spraying where the jets can now be tuned on demand.

[1] R. Bar-Ziv, T. Tlusty, E. Moses, S. A. Safran, and A. Bershadsky, Proc. Natl. Acad. Sci. U.S.A. **96**, 10140 (1999).
[2] F. Campelo and A. Hernández-Machado, Phys. Rev. Lett. **99**, 088101 (2007).
[3] A. Groisman and V. Steinberg, Nature (London) **405**, 53 (2000).
[4] J. de Jong, G. de Bruin, H. Reinten, M. van den Berg, H. Wijshoff, M. Versluis, and D. Lohse, J. Acoust. Soc. Am. **120**, 1257 (2006).
[5] O. A. Basaran, H. Gao, and P. P. Bhat, Annu. Rev. Fluid Mech. **45**, 85 (2013).
[6] B. Keshavarz, E. C. Houze, J. R. Moore, M. R. Koerner, and G. H. McKinley, Phys. Rev. Lett. **117**, 154502 (2016).

[7] Y. Amarouchene, D. Bonn, J. Meunier, and H. Kellay, Phys. Rev. Lett. **86**, 3558 (2001).
[8] G. H. McKinley, Rheol. Rev. (2005).
[9] F. Ingremeau and H. Kellay, Phys. Rev. X **3**, 041002 (2013).
[10] A. V. Bazilevskii, S. I. Voronkov, V. M. Entov, and A. N. Rozhkov, Sov. Phys. Dokl. **26**, 333 (1981).
[11] C. Clasen, J. Eggers, M. A. Fontelos, J. Lie, and G. h. McKinley, J. Fluid Mech. **556**, 283 (2006).
[12] C. Wagner, Y. Amarouchene, D. Bonn, and J. Eggers, Phys. Rev. Lett. **95**, 164504 (2005).
[13] M. Goldin, J. Yerushalmi, R. Pfeffer, and R. Shinnar, J. Fluid Mech. **38**, 689 (1969).
[14] V. M. Entov and a. L. Yarin, Fluid Dyn. **19**, 21 (1984).
[15] M. Stelter, G. Brenn, a. L. Yarin, R. P. Singh, and F. Durst, J. Rheol. **44**, 595 (2000).
[16] R. Sattler, C. Wagner, and J. Eggers, Phys. Rev. Lett. **100**, 164502 (2008).
[17] M. S. N. Oliveira and G. H. McKinley, Phys. Fluids **17**, 071704 (2005).
[18] R. Sattler, S. Gier, J. Eggers, and C. Wagner, Phys. Fluids **24**, 023101 (2012).
[19] P. P. Bhat, S. Appathurai, M. T. Harris, M. Pasquali, G. H. McKinley, and O. A. Basaran, Nat. Phys. **6**, 625 (2010).
[20] J. Eggers, Phys. Fluids **26**, 033106 (2014).
[21] J. Eggers, Rev. Mod. Phys. **69**, 865 (1997).
[22] A. A. Castrejon-Pita, J. R. Castrejon-Pita, and I. M. Hutchings, Phys. Rev. Lett. **108**, 074506 (2012).
[23] H. Stone, Annu. Rev. Fluid Mech. **26**, 65 (1994).
[24] F. S. Bates, Polymer-Polymer Phase Behavior (1991).
[25] R. Koningsveld, W. H. Stockmayer, and E. Nies, *Polymer Phase Diagrams: A Textbook* (Oxford University Press, Oxford, 2001).
[26] N. S. Berman, Annu. Rev. Fluid Mech. **10**, 47 (1978).
[27] A. Argumedo, T. T. Tung, and K. I. Chang, J. Rheol. **22**, 449 (1978).
[28] See Supplemental Material http://link.aps.org/supplemental/10.1103/PhysRevLett.120.194501 for details on the experimental setup and methods, details on the determination of the relaxation time, and effect of polymer concentration and temperature on the existence of the instabilities. It includes Refs. [29].
[29] V. Tirtaatmadja, H. G. McKinley, and J. J. Cooper-White, Phys. Fluids **18**, 043101 (2006).
[30] S. L. Anna and G. H. McKinley, J. Rheol. **45**, 115 (2001).
[31] A. Matsuyama and F. Tanaka, Phys. Rev. Lett. **65**, 341 (1990).
[32] A. Onuki, *Phase Transition Dynamics* (Cambridge University Press, Cambridge, 2002).
[33] M. Doi and S. F. Edwards, *The Theory of Polymer Dynamics* (Oxford University Press, Oxford, 1988), Vol. 73.
[34] F. C. Frank, A. Keller, and M. R. Mackley, Polymer **12**, 467 (1971).
[35] A. Onuki, Phys. Rev. Lett. **62**, 2472 (1989).